運用海嘯浮標預警系統之海床壓力計資料解析南海內孤立波特性

游千霈 、楊穎堅
國立臺灣大學海洋中心
潘琦
中央氣象署海象氣候組

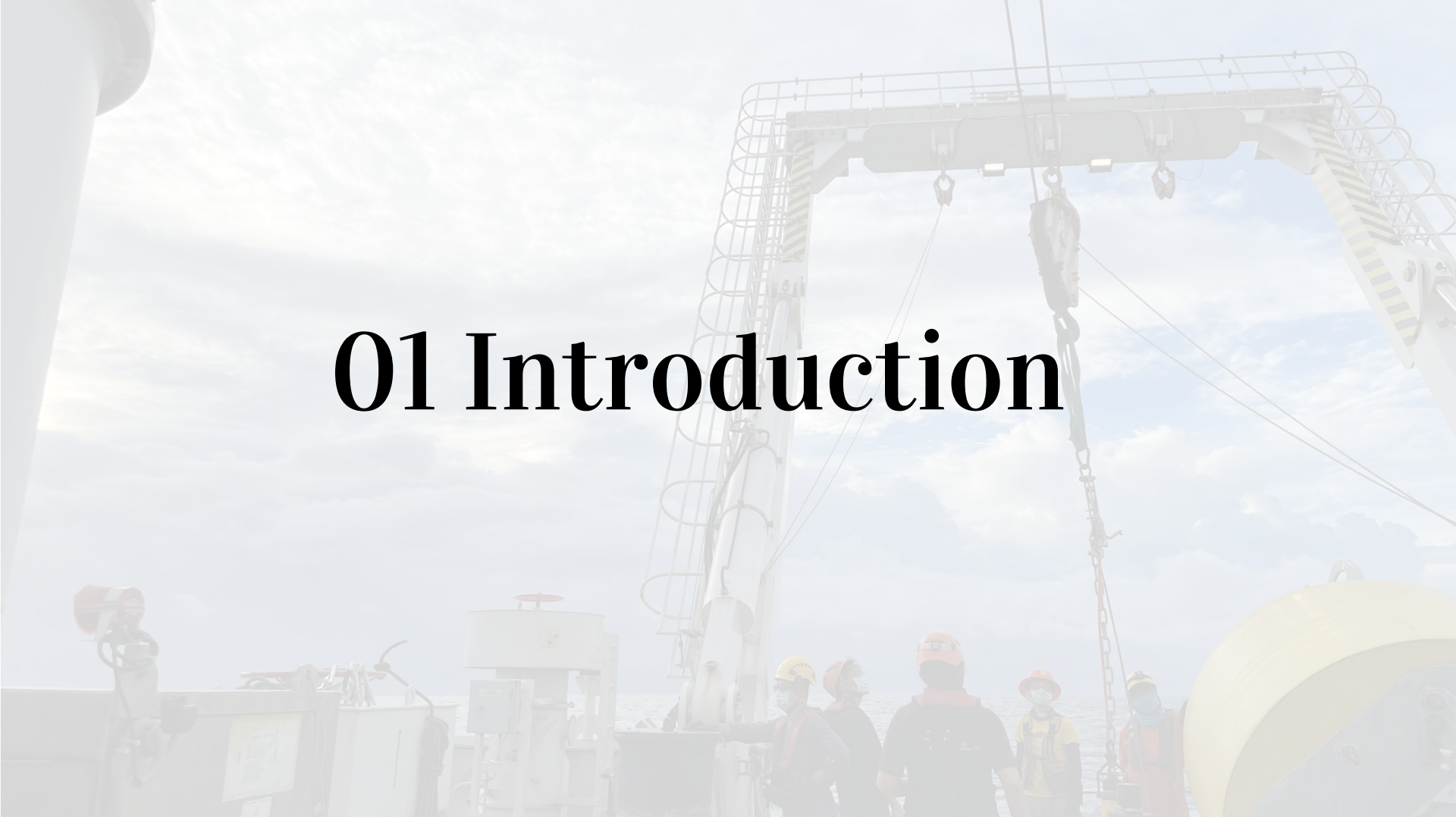

01 Introduction

Internal Waves in the SCS

(Alford et al., 2015)

Introduction

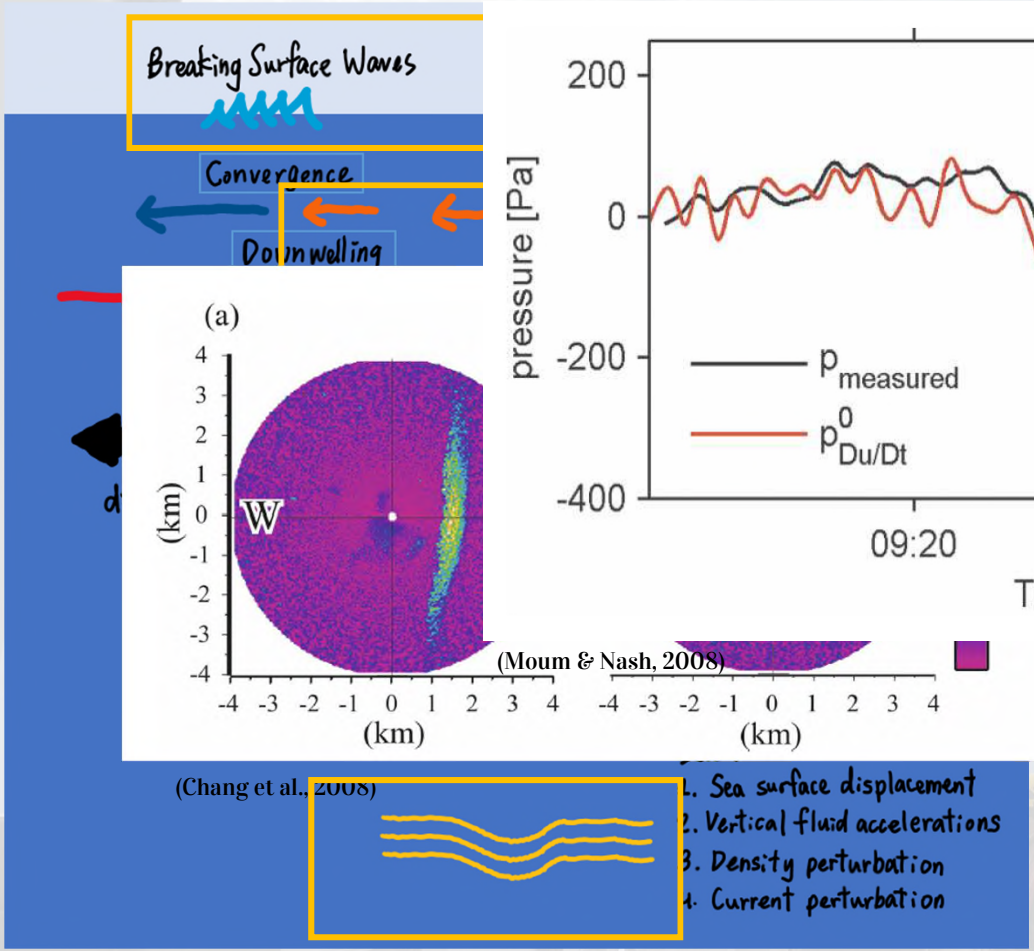

(Chang et al., 2008)

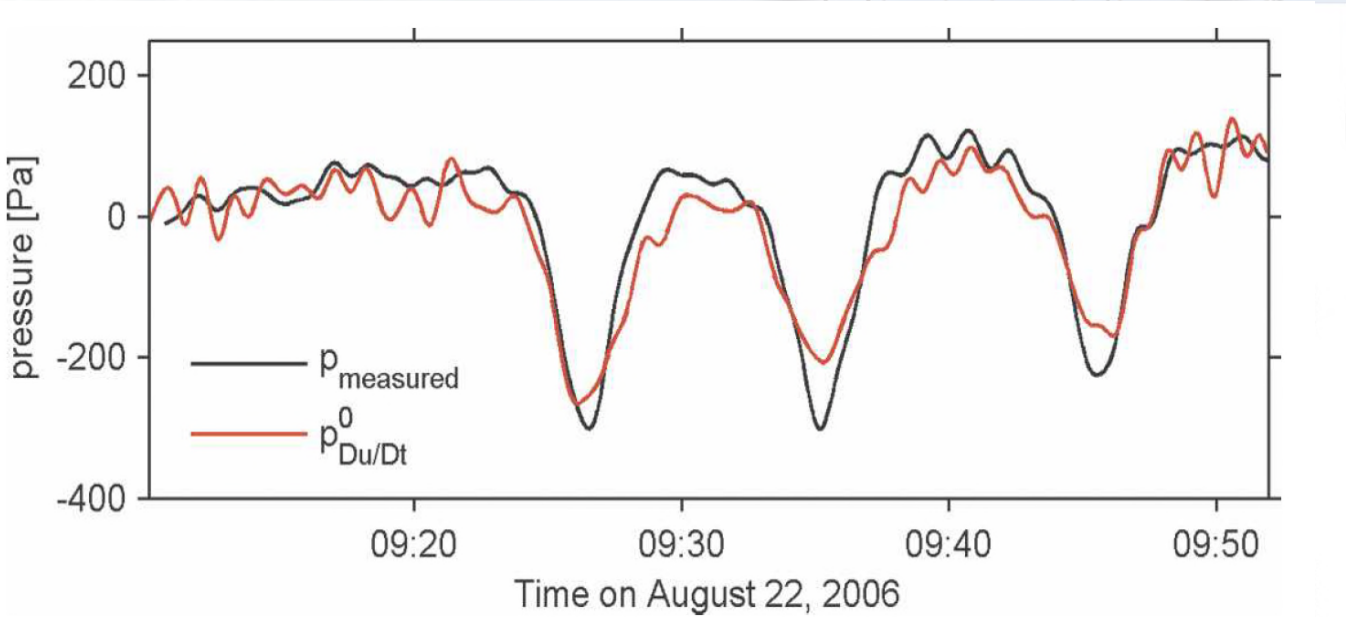

(Moum & Nash, 2008)

(Liu et al., 2004)

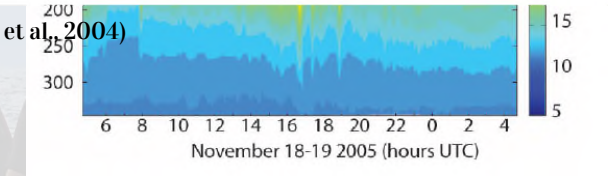

(Ramp et al., 2010)

Motivation and Goal

- Previous research on ISWs in the SCS, using various observation methods, yielded many results, but the duration was often short, and satellite imagery was frequently hindered by weather conditions.
- According to Moum et al. (2006 and 2008), the seafloor pressure perturbation caused by internal waves could be measured by pressure transducers in shallow water.
- This study aims to verify the feasibility of using deep ocean pressure measurements to document ISW.
- It compiles long-term ISW seasonal variations and uses the DJL method to find optimal internal wave properties, validated against observational data.

Tsunami Buoy and Bottom Pressure Recorder (BPR)

- Digiquartz® Transducer
- Typical application accuracy is better than 0.01% with 1/1,000,000,000 resolution (Paroscientific Inc., n.d.)
- Sensitive enough to measure a millimeter change in 6,000m (Lawson, 2013)

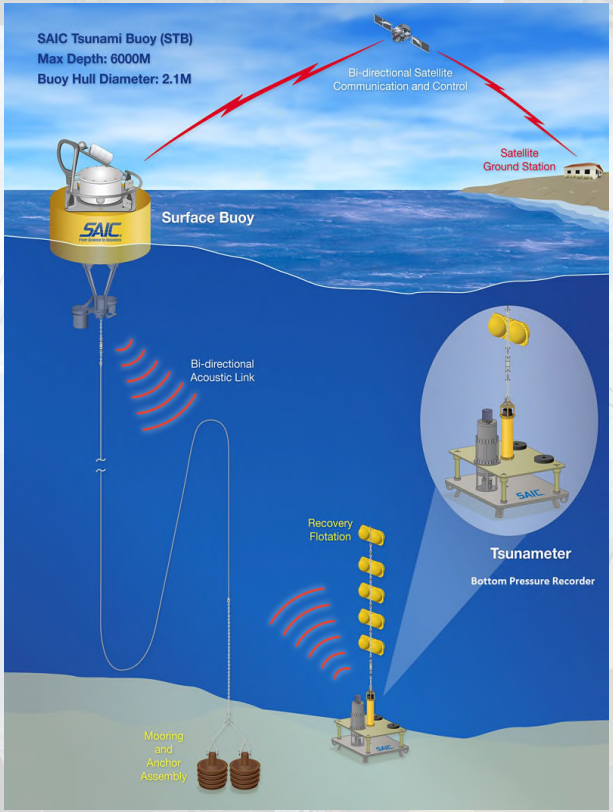

(Science Applications International Corporation, 2015)

Tsunami Buoy and Bottom Pressure Recorder (BPR)

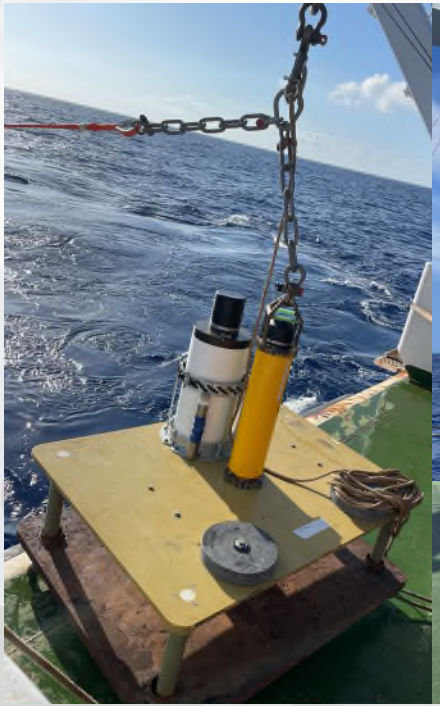

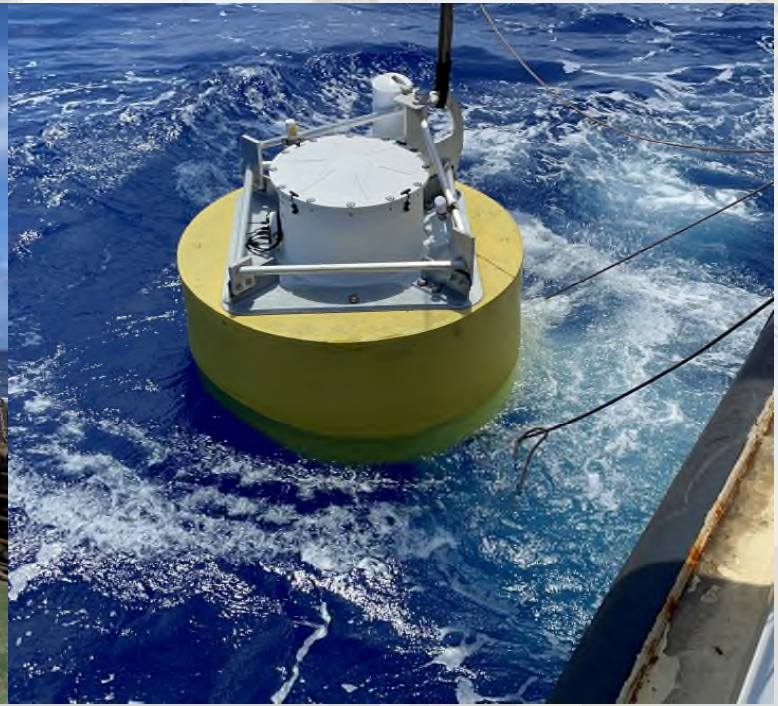

Introduction

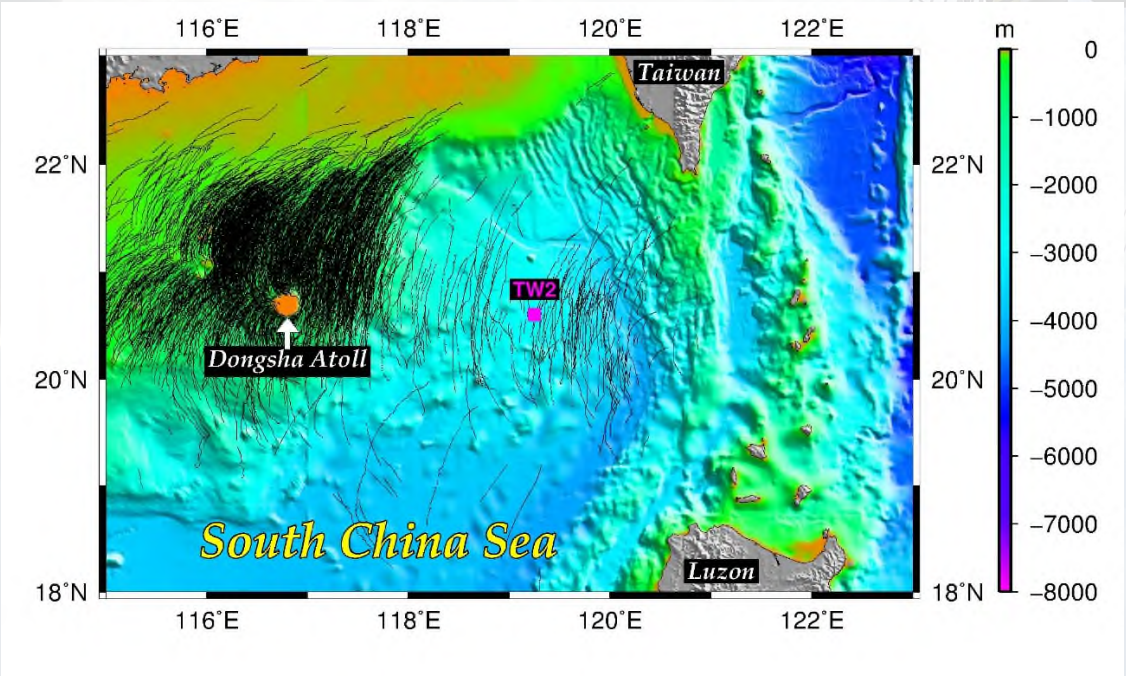

(Yang et al., 2009)

- Mooring Location: 119°14.4’E, 20°36’N
- Local water depth: ~2,800 m
- Observation period: 2.8 years (1,035 days)
- Sampling rate: 15 seconds converted to 1 minute

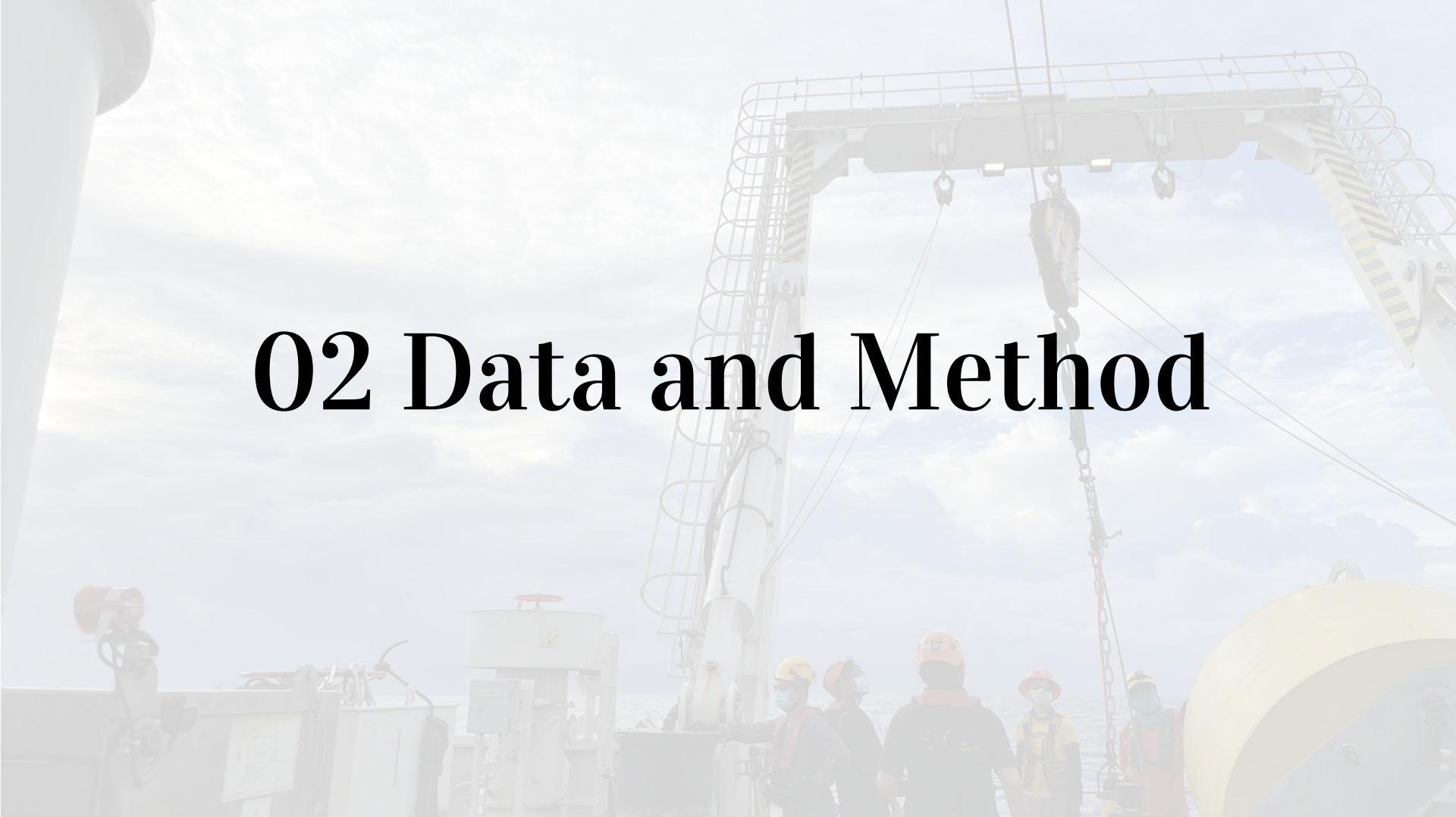

02 Data and Method

BPR Data

- Observation period: 2.8 years (1,035 days)
- Sampling rate: 15 seconds converted to 1 minute

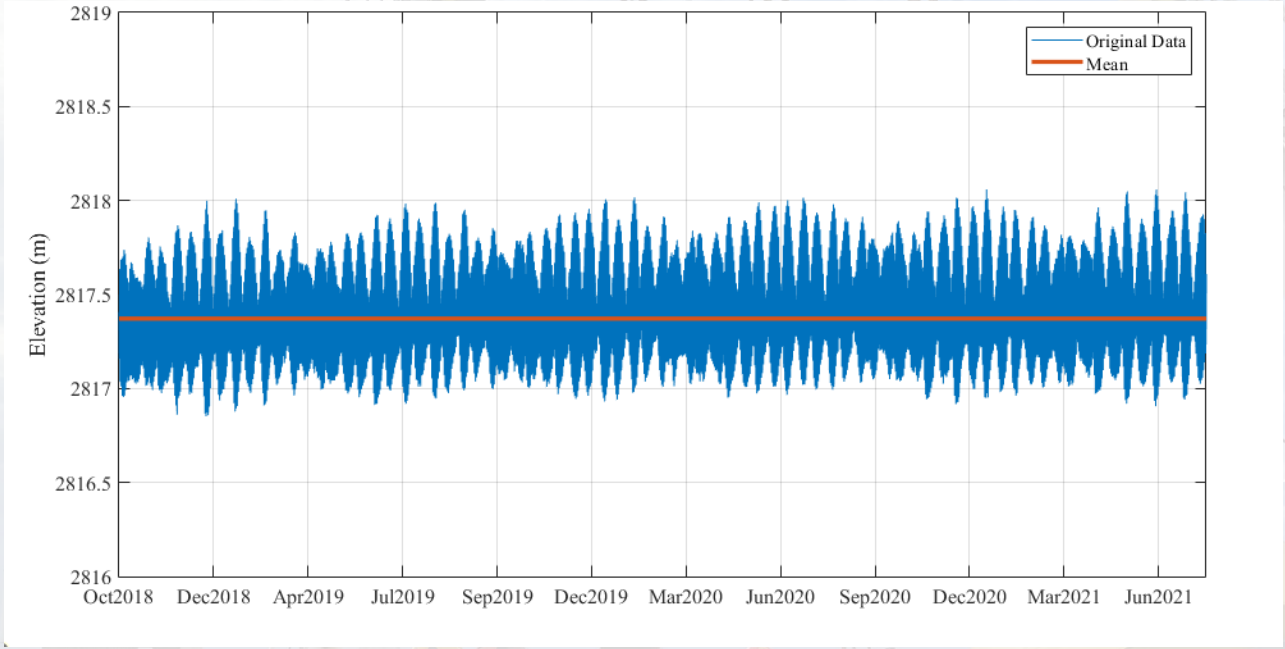

Internal Solitary Wave Data Source (Himawari-8)

- Wave length: 0.64 μm red band
- Spatial resolution: 0.5 km
- Sequence: 10 minutes
- This gridded data was distributed by the Center for Environmental Remote Sensing (CEReS), Chi-ba University, Japan (Higuchi et al., 2019; Takenaka et al., 2020; Yamamoto et al., 2020).

DJL Method

- The DJL method was used to enhance understanding of internal solitary wave dynamics. Dubreil-Jacotin-Long equation (Stastna, 2022):

$$\nabla^2\eta + \frac{U'(z-\eta)}{c-U(z-\eta)}(\eta_x^2 + (1-\eta_z)^2 - 1) + \frac{N^2(z-\eta)}{(c-U(z-\eta))^2}\eta = 0$$

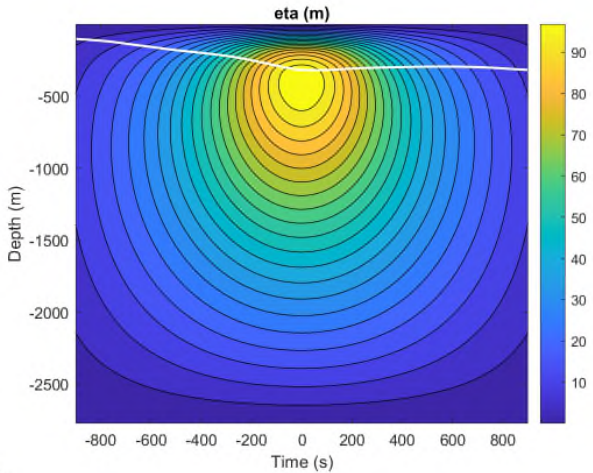

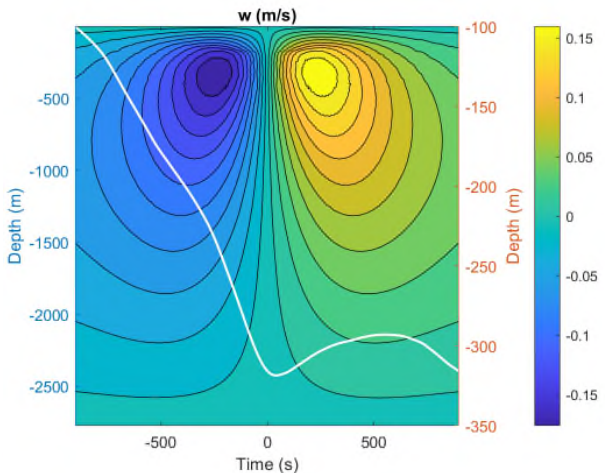

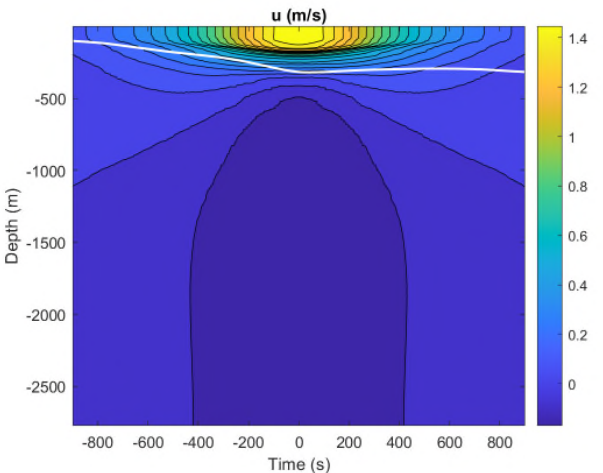

Background Density Data Sources

a) Seasonal data from the Seaglider

- Observation time: June 05, 2019

b) Historical data from the CTD sensor on research vessels

- Observation time:

1. CTD 1: May 25, 2008
2. CTD 2: October 14, 2024

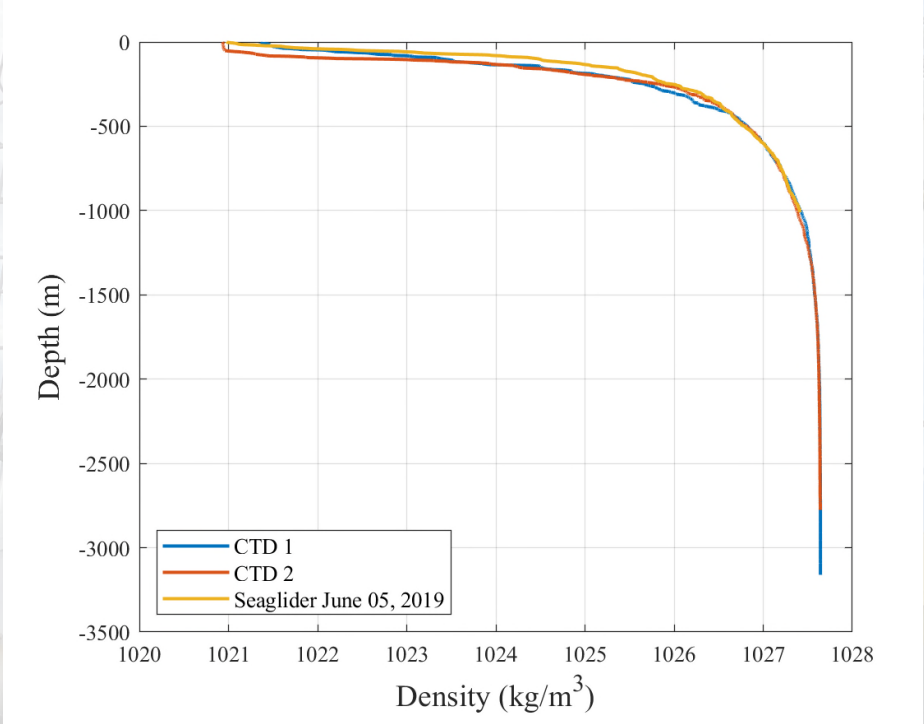

03 Results and Discussion

Tidal Constituents of the Observing Site

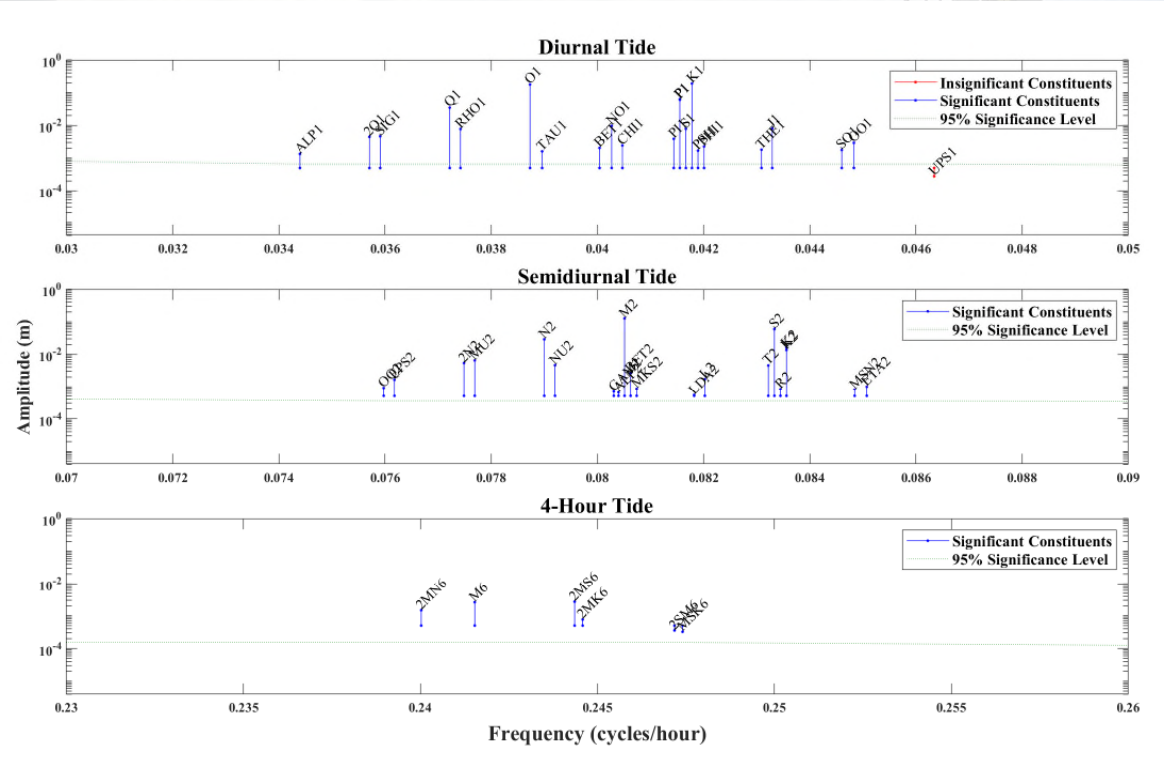

- $F = \frac{K_1+O_1}{M_2+S_2} = 1.96$
- Mixed, dominantly diurnal tides

CWT Results

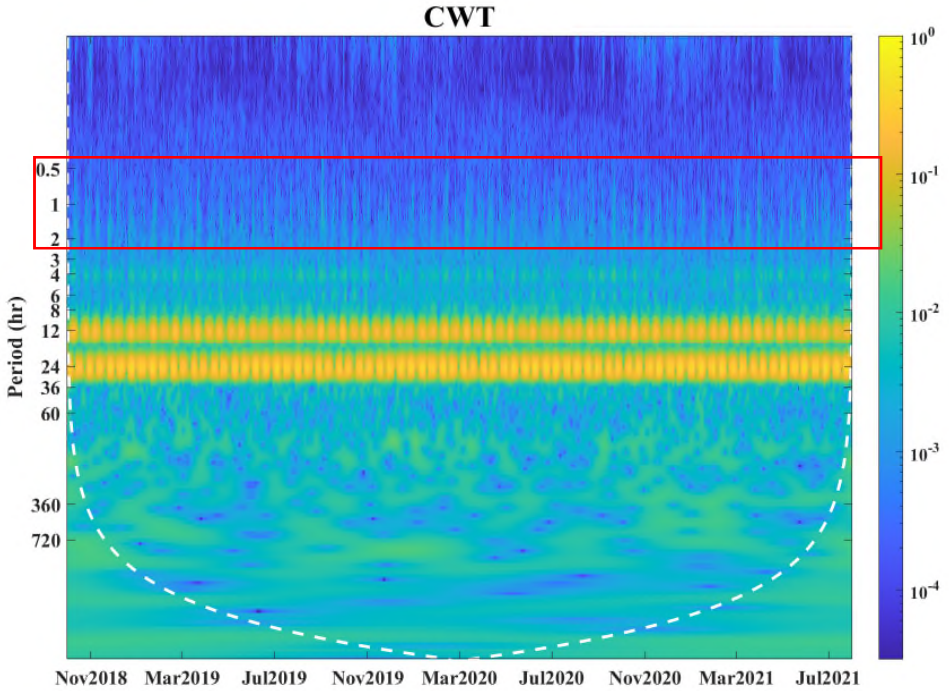
CWT
Period (hr)
0.5
1
2
3
4
6
8
12
24
36
60
360
720
Nov2018
Mar2019
Jul2019
Nov2019
Mar2020
Jul2020
Nov2020
Mar2021
Jul2021
10^{0}
10^{-1}
10^{-2}
10^{-3}
10^{-4}

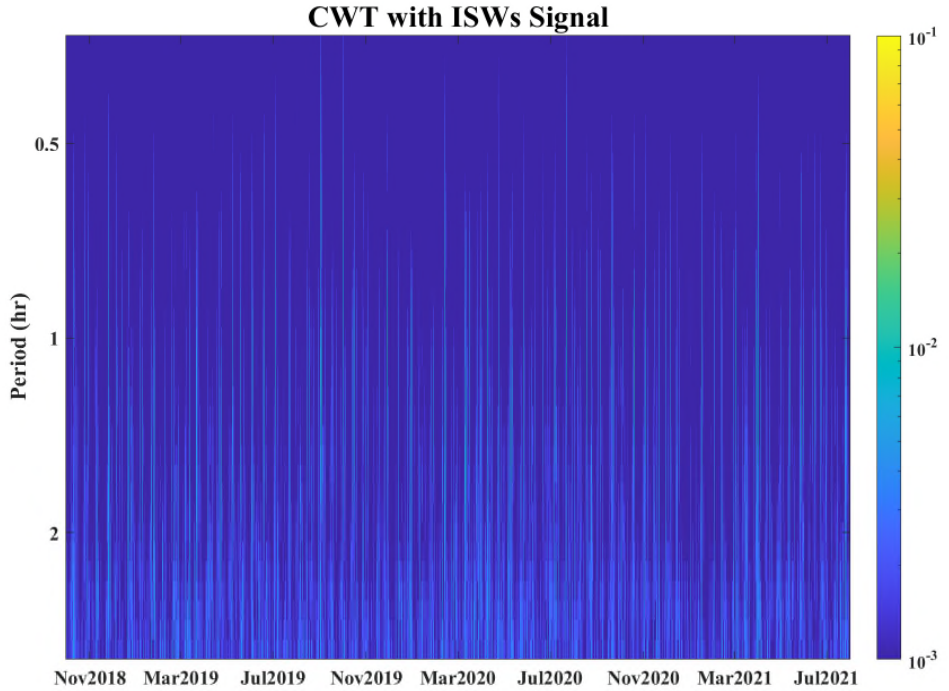
CWT with ISWs Signal
Period (hr)
0.5
1
2
Nov2018
Mar2019
Jul2019
Nov2019
Mar2020
Jul2020
Nov2020
Mar2021
Jul2021
10^{-1}
10^{-2}
10^{-3}

HHT Results

1-hour-period

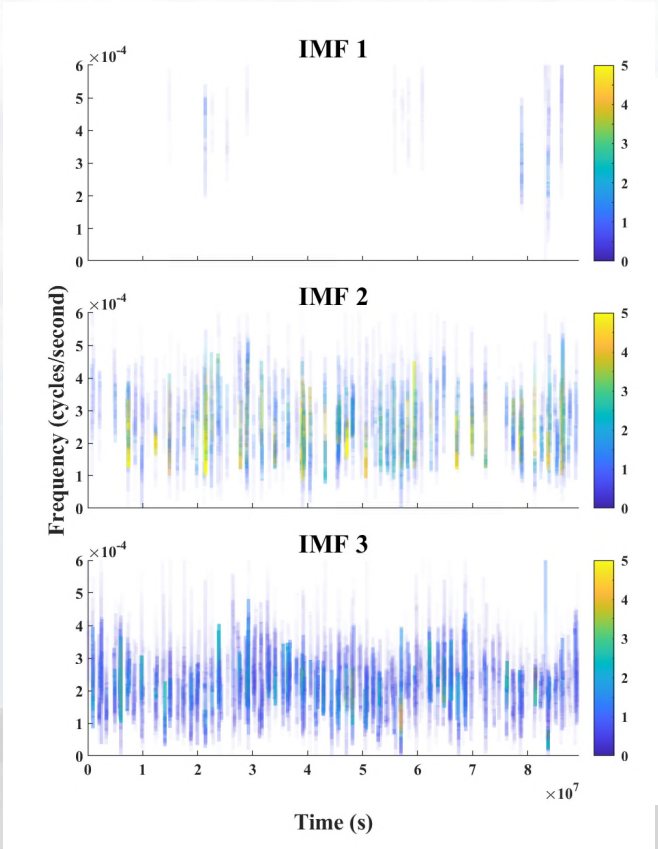

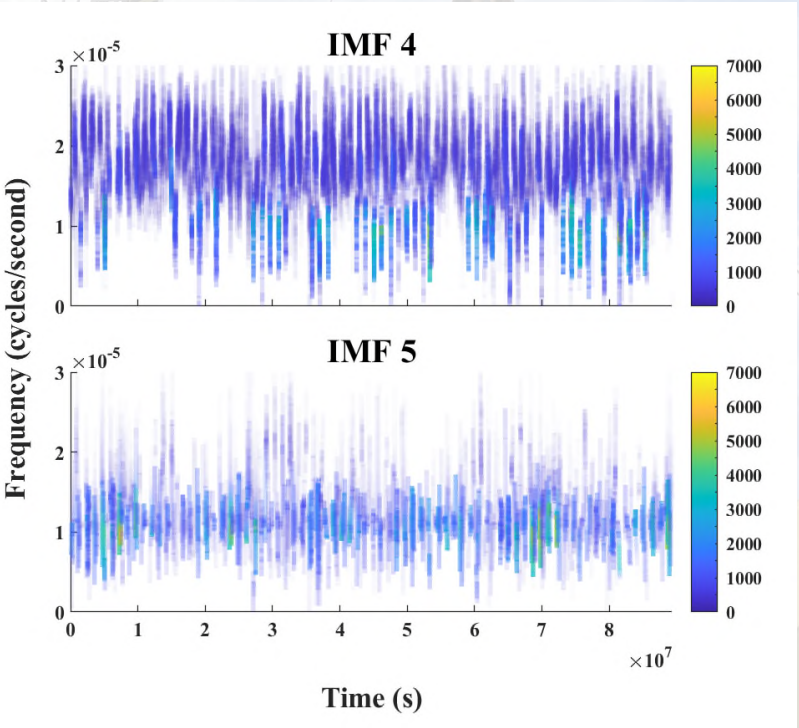

tide

Comparison of CWT Results and HHT Results

- The signal only appeared four days before and after the spring tide.
- The energy peaks matched with the perturbation on the de-tide data. As a result, IMF 1, 2, and 3 would be deemed as the perturbation induced by ISW traveling across the northern SCS.

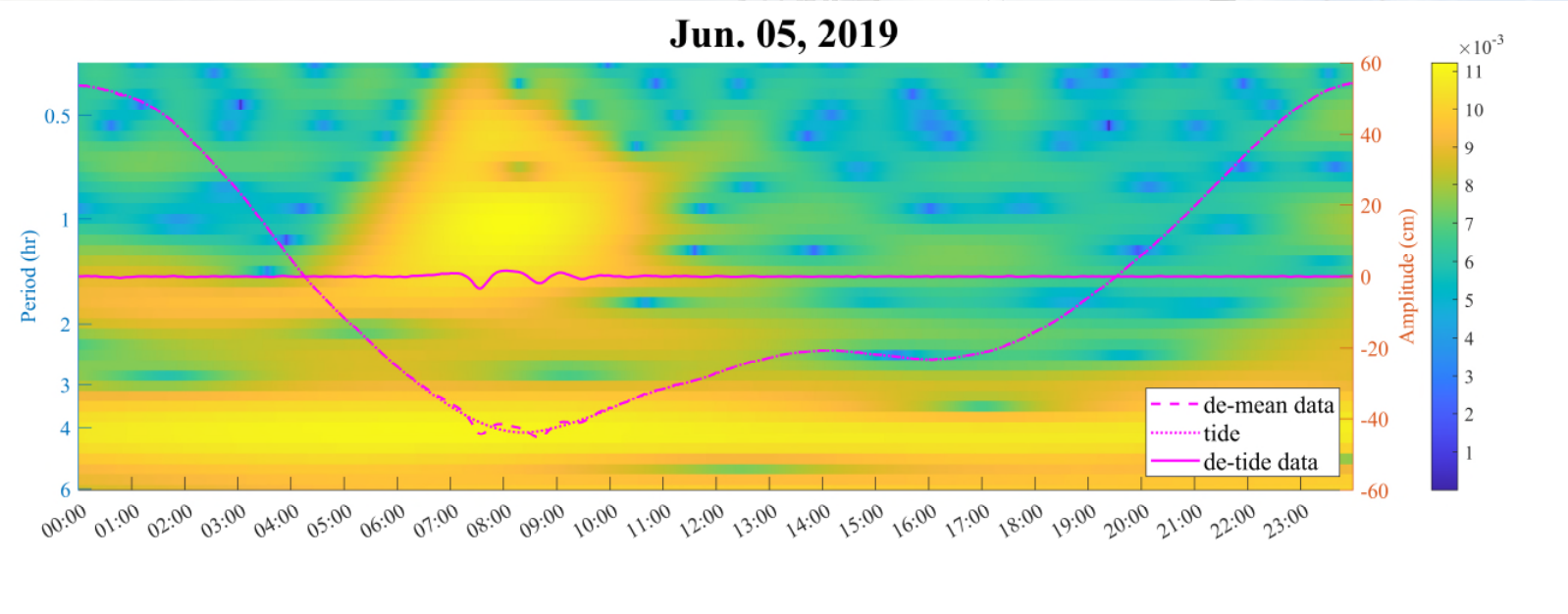

Statistical Results

- Total ISWs: 513 cases
  - Winter (Dec. to Feb.): 99
  - Spring (Mar. to May): 147
  - Summer (Jun. to Aug.): 135
  - Fall (Sep. to Nov.): 132
- 83.4% of ISWs have an amplitude between 0.5 to 2 cm
- The largest amplitude was recorded during Dec. 2019

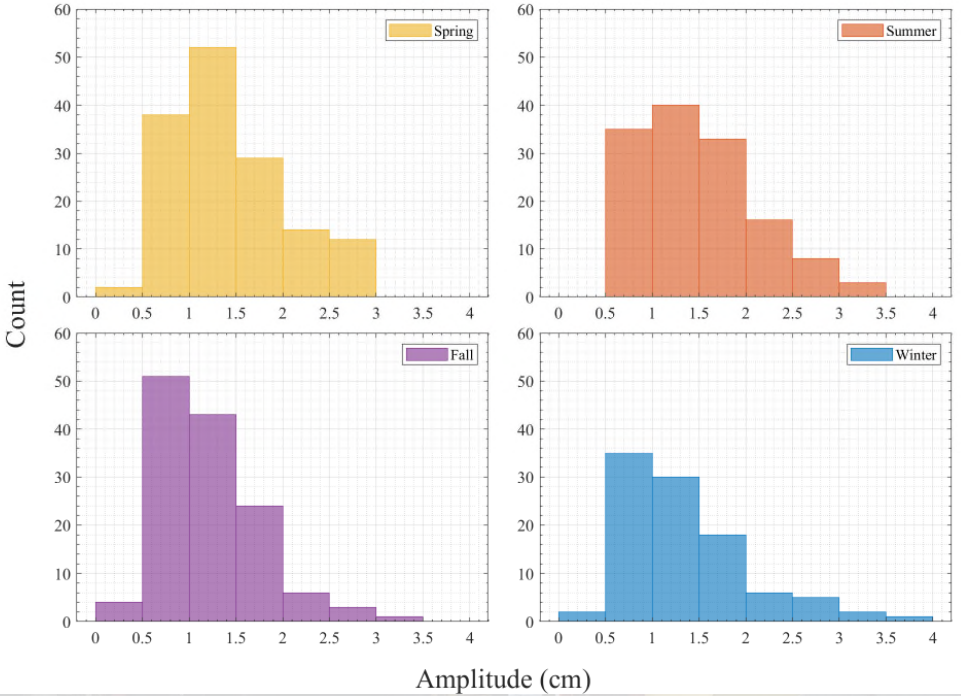

DJL Method with Seasonal Background Density Profile Application (Jun. 05, 2019)

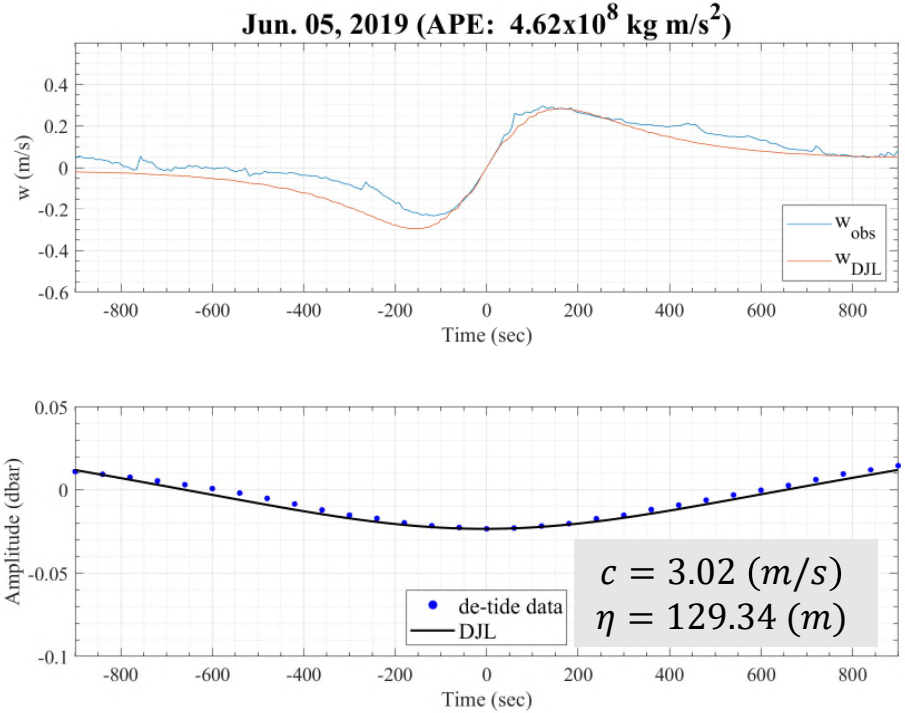

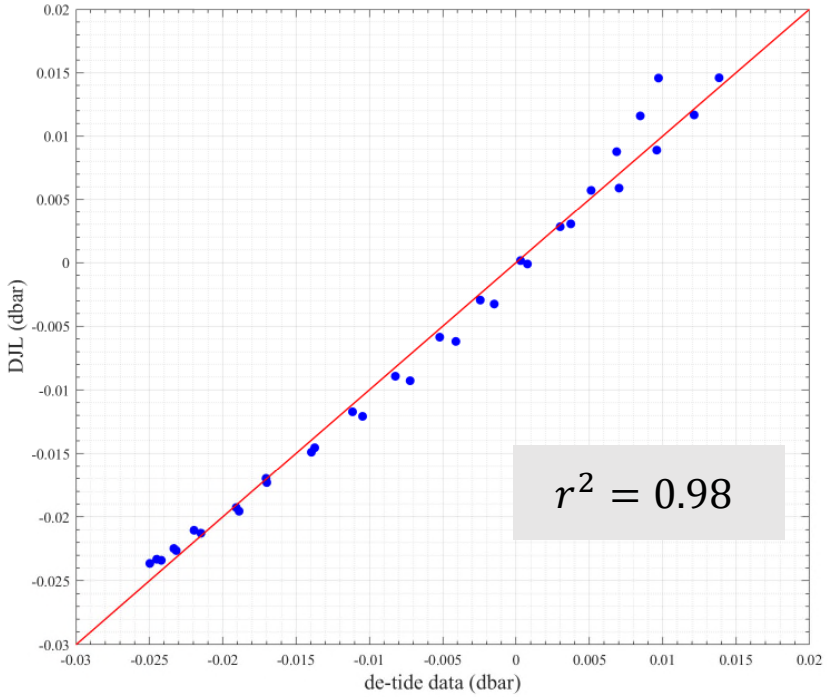

DJL Method with Historical Background Density Profile Application (Jun. 05, 2019)

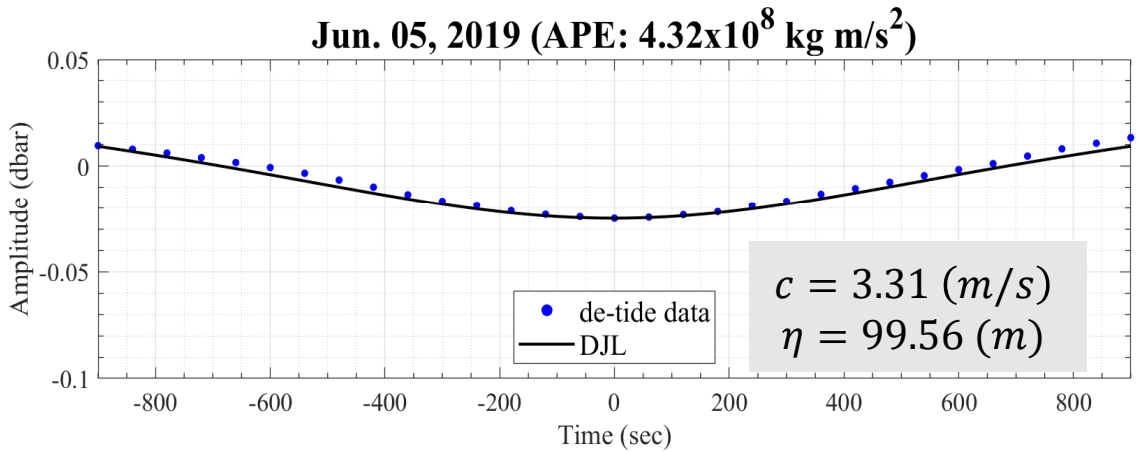

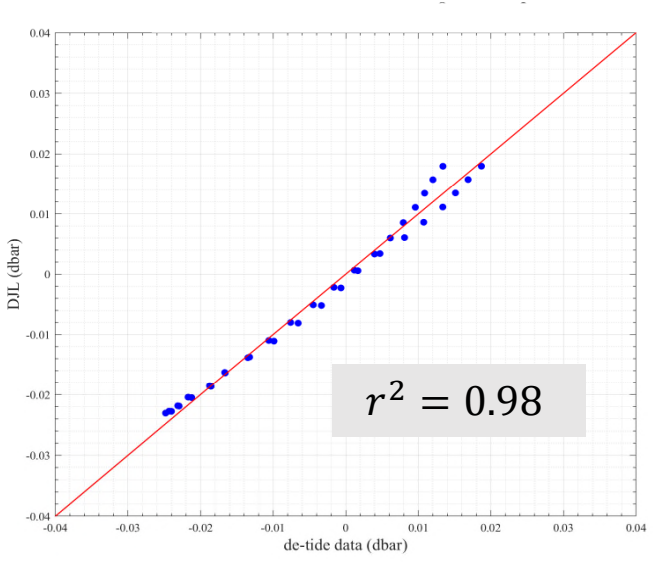

DJL Method with Historical Background Density Profile Application (Jun. 06, 2019)

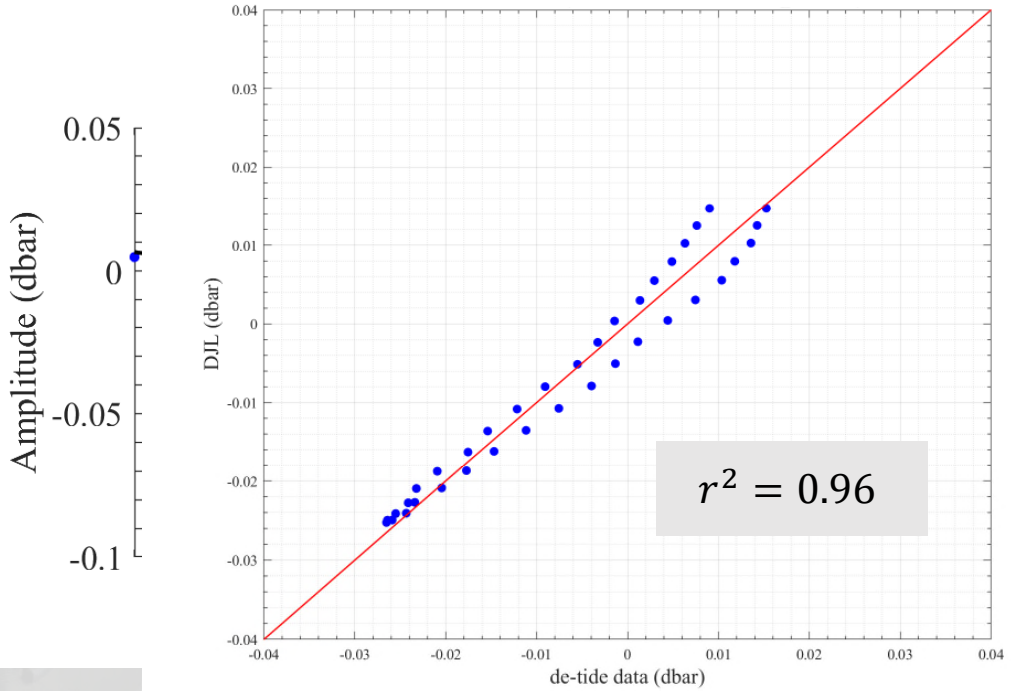

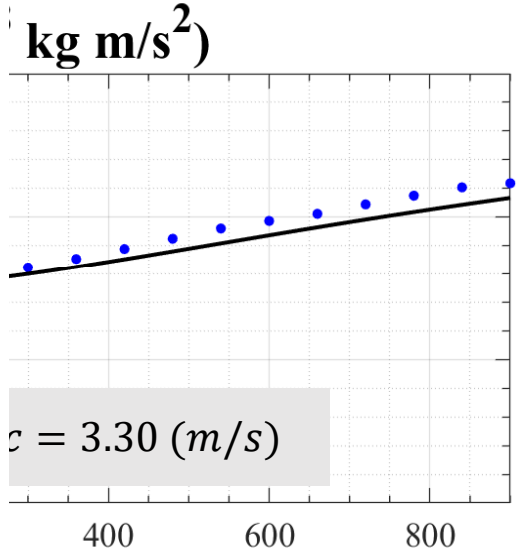

DJL Method with Historical Background Density Profile Application (Jun. 07, 2019)

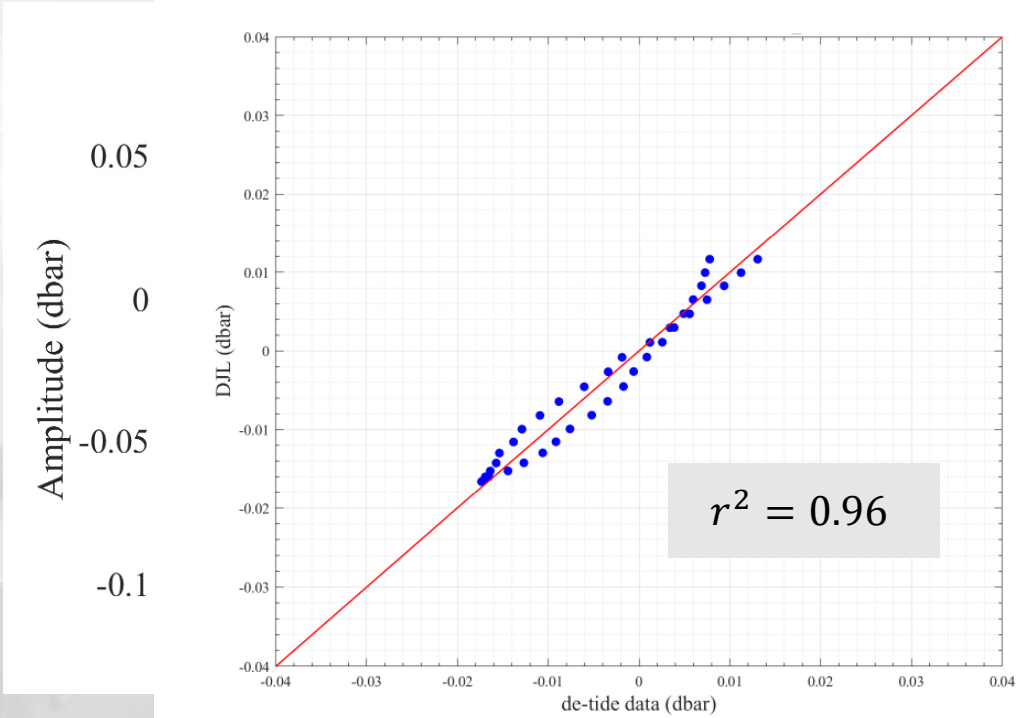

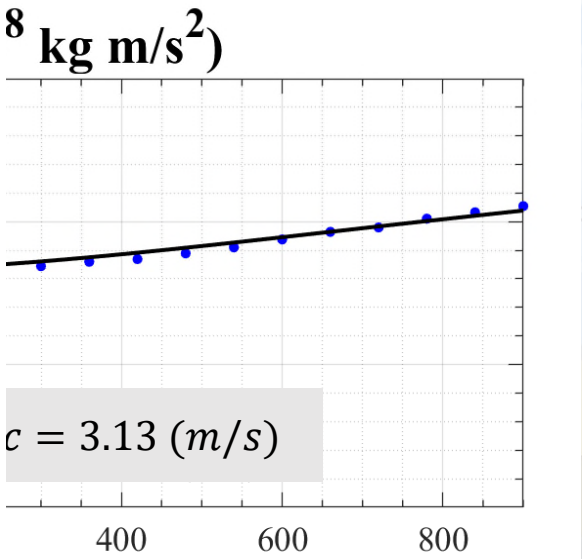

Himawari-8 Image (Jun. 05, 2019)

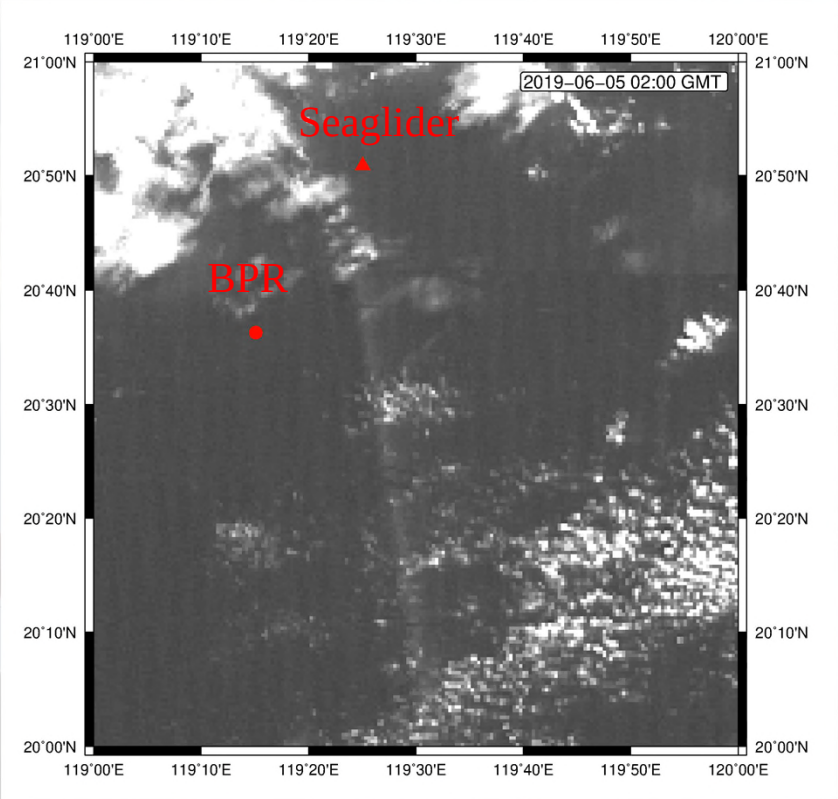

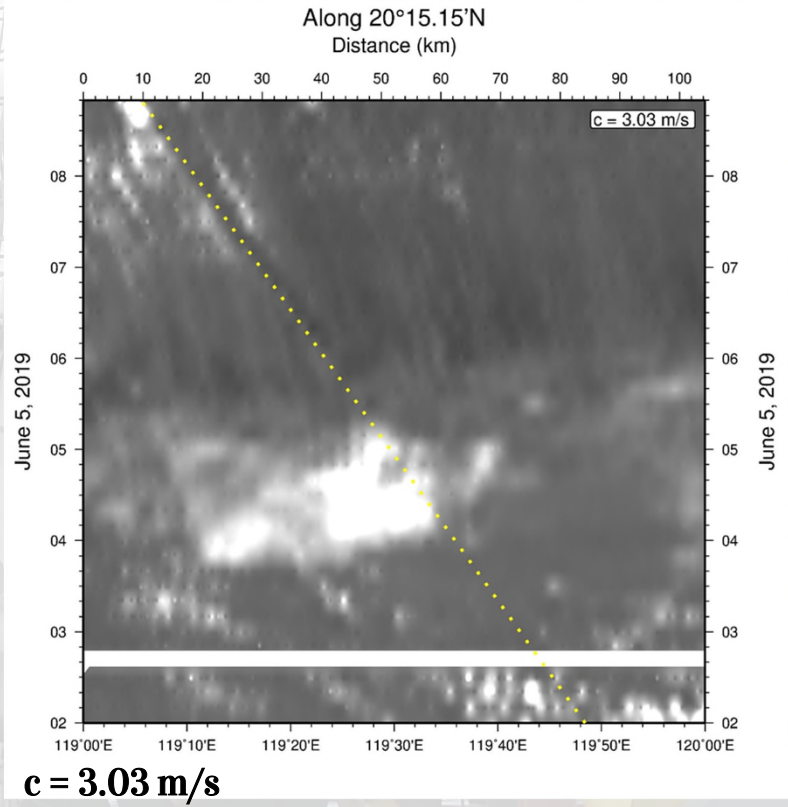

c = 3.03 m/s

Himawari-8 Image (Jun. 06, 2019)

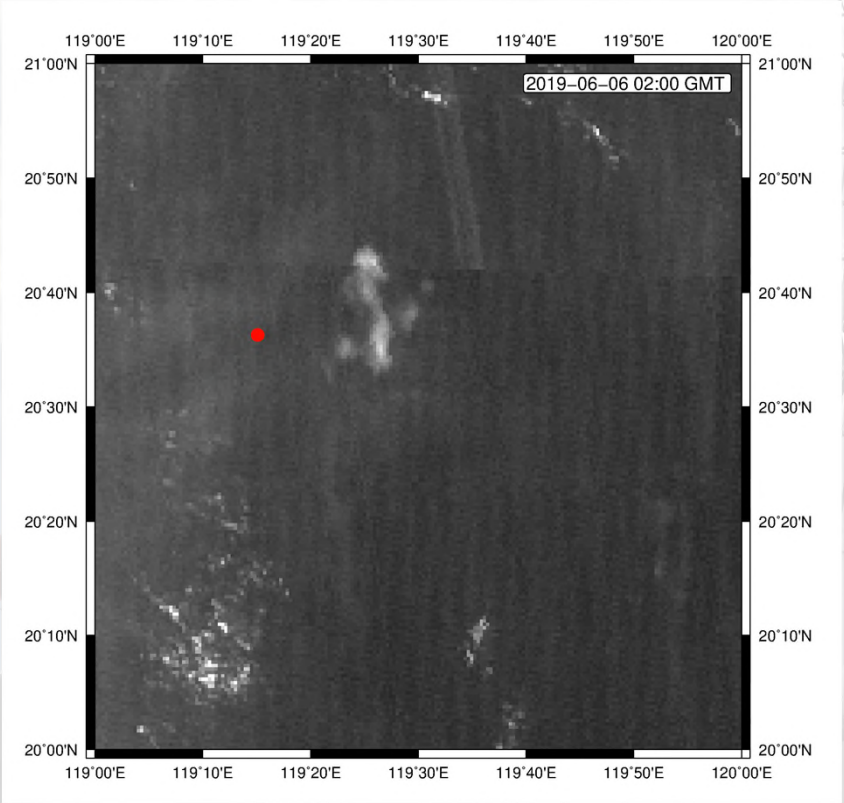

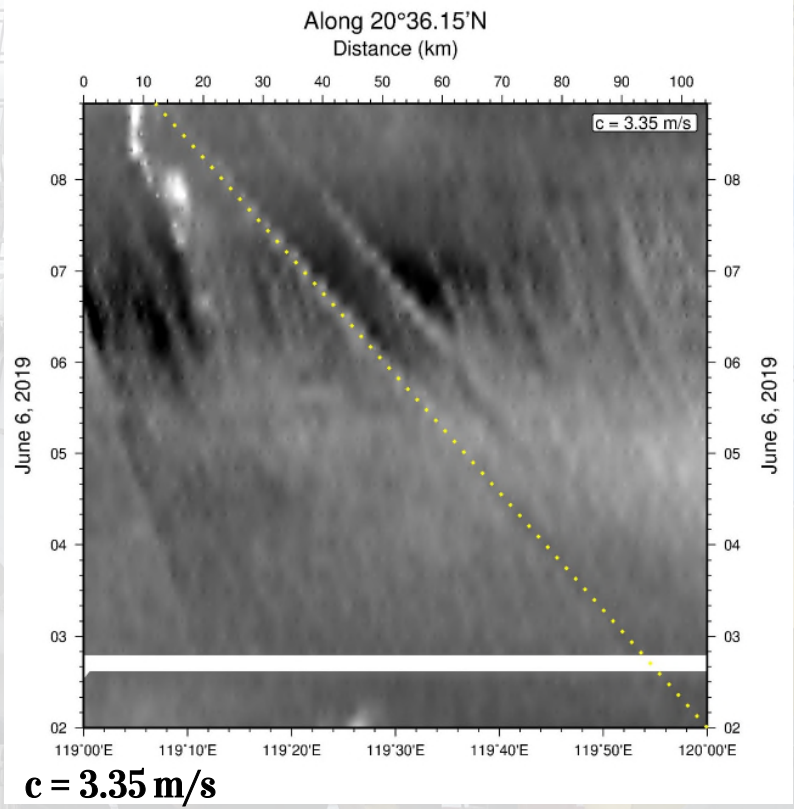

c = 3.35 m/s

Himawari-8 Image (Jun. 07, 2019)

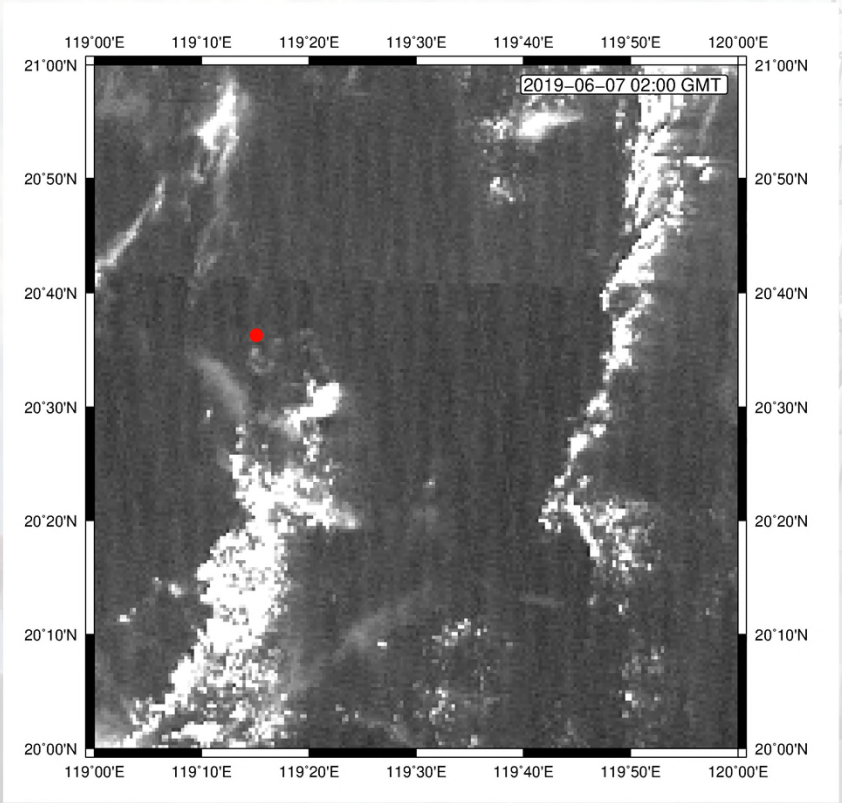

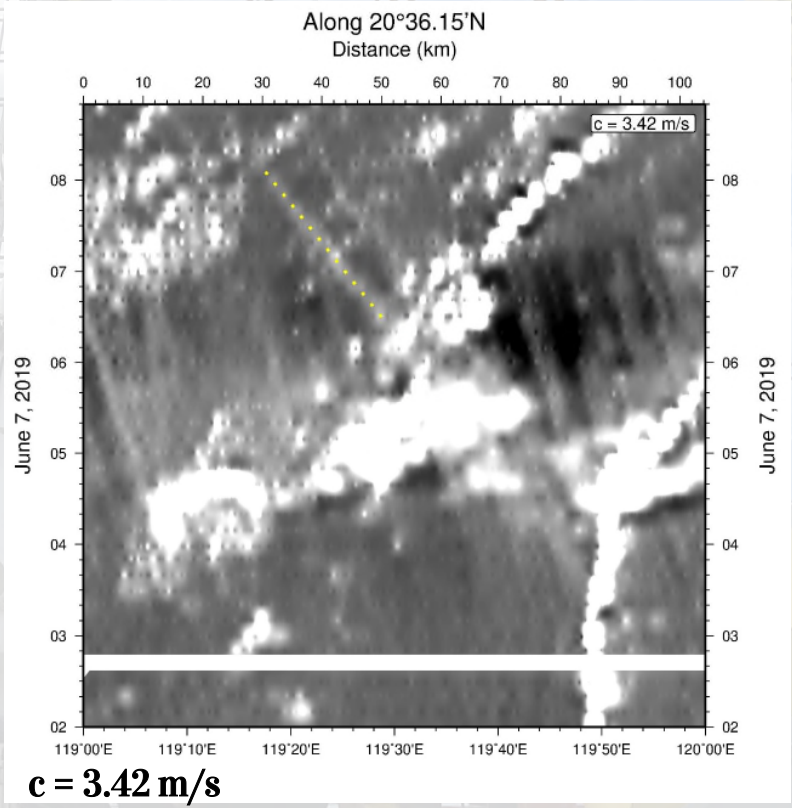

c = 3.42 m/s

Phase Speed *c (m/s)* Comparison

Case	Date	DJL Method	Himawari-8	Faster/ Slower
1	Jun. 05, 2019	3.02	3.03	-0.33%
2	Jun. 05, 2019	3.31	3.03	9.24%
3	Jun. 06, 2019	3.30	3.35	-1.49%
4	Jun. 07, 2019	3.13	3.42	-8.47%

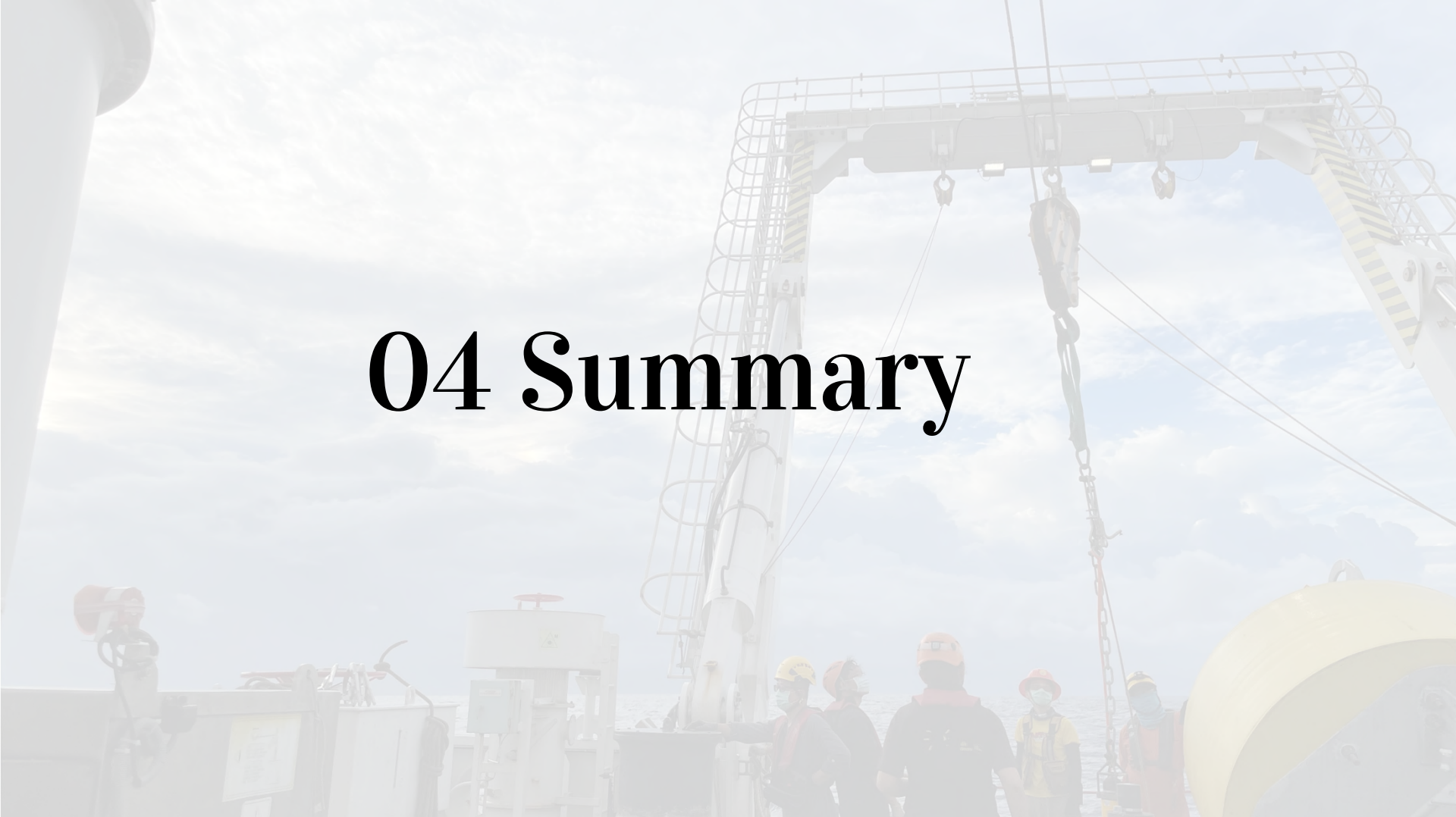

04 Summary

Summary

1. Pressure perturbations induced by internal solitary waves are detectable through BPRs in the deep basin.
2. ISW occurrences vary by season, with more events in spring, summer, and fall and fewer in winter, though wave amplitude remains unaffected by seasons.
3. The application of both seasonal and historical background density profiles in the DJL method showed highly accurate pressure results.
4. ISW generation is driven by stratification, so seasonal density profiles should be applied in the DJL method.

Research References

Alford, M. H., Lien, R.-C., Simmons, H., Klymak, J., Ramp, S., Yang, Y. J., Tang, D., & Chang, M.-H. (2010). Speed and Evolution of Nonlinear Internal Waves Transiting the South China Sea. Journal of Physical Oceanography, 40(6), 1338-1355. https://doi.org/10.1175/2010JPO4388.1

Alford, M. H., Peacock, T., MacKinnon, J. A., Nash, J. D., Buijsman, M. C., Centurioni, L. R., Chao, S. Y., Chang, M. H., Farmer, D. M., Fringer, O. B., Fu, K. H., Gallacher, P. C., Graber, H. C., Helfrich, K. R., Jachec, S. M., Jackson, C. R., Klymak, J. M., Ko, D. S., Jan, S., . . . Tang, T. Y. (2015). The Formation and Fate of Internal Waves in the South China Sea. Nature, 521(7550), 65-69. https://doi.org/10.1038/nature14399

Chang, M.-H., Cheng, Y.-H., Yang, Y. J., Jan, S., Ramp, S. R., Reeder, D. B., Hsieh, W.-T., Ko, D. S., Davis, K. A., Shao, H.-J., & Tseng, R.-S. (2021). Direct Measurements Reveal Instabilities and Turbulence within Large Amplitude Internal Solitary Waves beneath the Ocean. Communications Earth & Environment, 2(1). https://doi.org/10.1038/s43247-020-00083-6

Chang, M.-H., Lien, R.-C., Yang, Y. J., & Tang, T. Y. (2011). Nonlinear Internal Wave Properties Estimated with Moored Adcp Measurements. Journal of Atmospheric and Oceanic Technology, 28(6), 802-815. https://doi.org/10.1175/2010jtecho814.1

Chang, M.-H., Lien, R.-C., Yang, Y. J., Tang, T. Y., & Wang, J. (2008). A Composite View of Surface Signatures and Interior Properties of Nonlinear Internal Waves: Observations and Applications. Journal of Atmospheric and Oceanic Technology, 25(7), 1218-1227. https://doi.org/10.1175/2007jtecho574.1

Farmer, D., Alford, M., Lien, R.-C., Yang, Y. J., Chang, M.-H., & Li, Q. (2011). From Luzon Strait to Dongsha Plateau: Stages in the Life of an Internal Wave. Oceanography, 24(4), 64-77. https://doi.org/10.5670/oceanog.2011.95

Farmer, D., Li, Q., & Park, J. H. (2009). Internal Wave Observations in the South China Sea: The Role of Rotation and Non-Linearity. Atmosphere-Ocean, 47(4), 267-280. https://doi.org/10.3137/oc313.2009

Higuchi, A., Takenaka, H., & Toyoshima, K. (2019). Himawari 8/9 Gridded Full-Disk (Fd)Data Version 02 (V20190123) ([Gridded Data]. Center for Environmental Remote Sensing (CEReS), Chiba University. ftp://hmwr829gr.cr.chiba-u.ac.jp/gridded/FD/V20190123/

Jackson, C. R. (2009). An Empirical Model for Estimating the Geographic Location of Nonlinear Internal Solitary Waves. Journal of Atmospheric and Oceanic Technology, 26(10), 2243-2255. https://doi.org/10.1175/2009JTECHO638.1

Lawson, R. (2013). Saic Tsunami Buoy (Stb) and Easy-to-Deploy (Etd) Dart® Systems. In: Science Applications International Corporation (SAIC).

Li, Q., & Farmer, D. M. (2011). The Generation and Evolution of Nonlinear Internal Waves in the Deep Basin of the South China Sea. Journal of Physical Oceanography, 41(7), 1345-1363. https://doi.org/10.1175/2011JPO4587.1

Liu, A. K., Ramp, S. R., Zhao, Y., & Tang, T. Y. (2004). A Case Study of Internal Solitary Wave Propagation during Asiaex 2001. IEEE Journal of Oceanic Engineering, 29(4), 1144-1156. https://doi.org/10.1109/joe.2004.841392

Moum, J. N., & Nash, J. D. (2008). Seafloor Pressure Measurements of Nonlinear Internal Waves. Journal of Physical Oceanography, 38(2), 481-491. https://doi.org/10.1175/2007jpo3736.1

Moum, J. N., & Smyth, W. D. (2006). The Pressure Disturbance of a Nonlinear Internal Wave Train. Journal of Fluid Mechanics, 558. https://doi.org/10.1017/s0022112006000036

Orr, M. H., & Mignerey, P. C. (2003). Nonlinear Internal Waves in the South China Sea: Observation of the Conversion of Depression Internal Waves to Elevation Internal Waves. Journal of Geophysical Research: Oceans, 108(C3). https://doi.org/10.1029/2001JC001163

Paroscientific Inc. (n.d.). D25 Series 2000, 3000, 4000: Absolute and Gauge Pressure Transducers. In: Paroscientific Inc.

Ramp, S. R., Park, J. H., Yang, Y. J., Bahr, F. L., & Jeon, C. (2019). Latitudinal Structure of Solitons in the South China Sea. Journal of Physical Oceanography, 49(7), 1747-1767. https://doi.org/10.1175/jpo-d-18-0071.1

Ramp, S. R., Tang, T. Y., Duda, T. F., Lynch, J. F., Liu, A. K., Chiu, C. S., Bahr, F. L., Kim, H. R., & Yang, Y. J. (2004). Internal Solitons in the Northeastern South China Sea Part I: Sources and Deep Water Propagation. IEEE Journal of Oceanic Engineering, 29(4), 1157-1181. https://doi.org/10.1109/joe.2004.840839

Ramp, S. R., Yang, Y. J., & Bahr, F. L. (2010). Characterizing the Nonlinear Internal Wave Climate in the Northeastern South China Sea. Nonlinear Processes in Geophysics, 17(5), 481-498. https://doi.org/10.5194/npg-17-481-2010

Stastna, M. (2022). Internal Waves in the Ocean (S. o. E. Michael Brenner, Harvard University, Cambridge, USA, E. L. Gábor Csányi, University of Cambridge, Cambridge, UK, S. o. E. Lakshminarayanan Mahadevan, Harvard University, Cambridge, USA, M. D. Clarence Rowley, Princeton University, Princeton, USA, F. H. Amit Singer, Princeton University, Princeton, USA, W. C. M. C. Jonathon D Victor, New York, USA, D. o. M. Rachel Ward, Office 10.144, University of Texas at Austin, & O. Dept of Mathematics, Austin, USA, Eds. 1 ed., Vol. 9). Springer Cham. https://doi.org/10.1007/978-3-030-99210-1

Takenaka, H., Sakashita, T., Higuchi, A., & Nakajima, T. (2020). Geolocation Correction for Geostationary Satellite Observations by a Phase-Only Correlation Method Using a Visible Channel. Remote Sensing, 12(15), 2472. https://www.mdpi.com/2072-4292/12/15/2472

Yamamoto, Y., Ichii, K., Higuchi, A., & Takenaka, H. (2020). Geolocation Accuracy Assessment of Himawari-8/Ahi Imagery for Application to Terrestrial Monitoring. Remote Sensing, 12(9), 1372. https://www.mdpi.com/2072-4292/12/9/1372

Yang, K.-C., Jan, S., Yang, Y. J., Chang, M.-H., Wang, J., Wang, S.-H., Ramp, S. R., Reeder, D. B., & Ko, D. S. (2023). Anatomy of Mode-1 Internal Solitary Waves Derived from Seaglider Observations in the Northern South China Sea. Journal of Physical Oceanography, 53(11), 2519-2536. https://doi.org/10.1175/jpo-d-23-0039.1

Yang, Y. J., Tang, T. Y., Chang, M. H., Liu, A. K., Hsu, M. K., & Ramp, S. R. (2004). Solitons Northeast of Tung-Sha Island during the Asiaex Pilot Studies. IEEE Journal of Oceanic Engineering, 29(4), 1182-1199. https://doi.org/10.1109/joe.2004.841424